2001

Earthquake stress drop and laboratory-inferred interseismic strength recovery

N. M. Beeler
U.S. Geological Survey

S. H. Hickman
U.S. Geological Survey

T. F. Wong
State University of New York

JOURNAL OF GEOPHYSICAL RESEARCH, VOL. 106, NO. B12, PAGES 30,701–30,713, DECEMBER 10, 2001

Earthquake stress drop and laboratory-inferred interseismic strength recovery

N. M. Beeler and S. H. Hickman
United States Geological Survey, Menlo Park, California

T.-f. Wong
Department of Geosciences, State University of New York

Abstract. We determine the scaling relationships between earthquake stress drop and recurrence interval t_r that are implied by laboratory-measured fault strength. We assume that repeating earthquakes can be simulated by stick-slip sliding using a spring and slider block model. Simulations with static/kinetic strength, time-dependent strength, and rate- and state-variable-dependent strength indicate that the relationship between loading velocity and recurrence interval can be adequately described by the power law $V_L \propto t_r^n$, where n=-1. Deviations from n=-1 arise from second order effects on strength, with n>-1 corresponding to apparent time-dependent strengthening and n<-1 corresponding to weakening. Simulations with rate and state-variable equations show that dynamic shear stress drop $\Delta\tau_d$ scales with recurrence as $d\Delta\tau_d/d\ln t_r \le \sigma_e(b-a)$, where σ_e is the effective normal stress, $\mu=\tau/\sigma_e$, and $(a\text{-}b)=d\mu_{ss}/d\ln V$ is the steady-state slip rate dependence of strength. In addition, accounting for seismic energy radiation, we suggest that the static shear stress drop $\Delta\tau_s$ scales as $d\Delta\tau_s/d\ln t_r \le \sigma_e(1+\zeta)(b-a)$, where ζ is the fractional overshoot. The variation of $\Delta\tau_s$ with $\ln t_r$ for earthquake stress drops is somewhat larger than implied by room temperature laboratory values of ζ and b-a. However, the uncertainty associated with the seismic data is large and the discrepancy between the seismic observations and the rate of strengthening predicted by room temperature experiments is less than an order of magnitude.

1. Introduction

For an earthquake to recur following stress drop, the fault must restrengthen during the interseismic period [*Brace and Byerlee*, 1966]. Faults that are stressed continuously by tectonic forces and which exhibit systematic variations in stress drop with recurrence interval may be used to infer the rate of interseismic restrengthening. For example, increases in static shear stress drop, which is defined as the difference between the failure strength (initial stress) and the residual stress $\Delta\tau_s=\tau_f-\tau_o$ (Figure 1), with recurrence interval would directly reflect time-dependent changes in failure strength, provided that the residual stress is independent of recurrence interval. Such recurrence-dependent stress drops are observed for some large (M 5.5-7.5) crustal earthquakes [*Kanamori and Allen*, 1986; *Scholz et al.*, 1986; *Scholz*, 1990]. In these studies, the static stress drop is calculated using seismic moment measured from seismograms and from estimated rupture area, while recurrence interval is estimated from historic records. The relative change in static stress drop per decade increase in recurrence for these large earthquakes is typically 2-3 MPa/decade [*Cao and Aki*, 1986, Figure 1; *Scholz*, 1990, Table 6.2). Some repeating small earthquakes, for example a M~1.5 along the Calaveras fault in central California (CA1) [*Vidale et al.*, 1994; *Marone et al.*, 1995], have stress drops that increase with recurrence at a rate comparable to large earthquakes (Figure 2). For these small repeating events, recurrence interval is measured directly and relative moment is determined using seismograms recorded at a large number of nearby stations. At least for the CA1 recurring event on the Calaveras fault, stress drop can be estimated from the relative moment and event duration [*Vidale et al.*, 1994; *Marone et al.*, 1995]. *Marone* [1998a, 1998b] compiled the stress drop observations from small and large events and, again presuming that the residual stress is independent of recurrence, concluded that strengthening rates

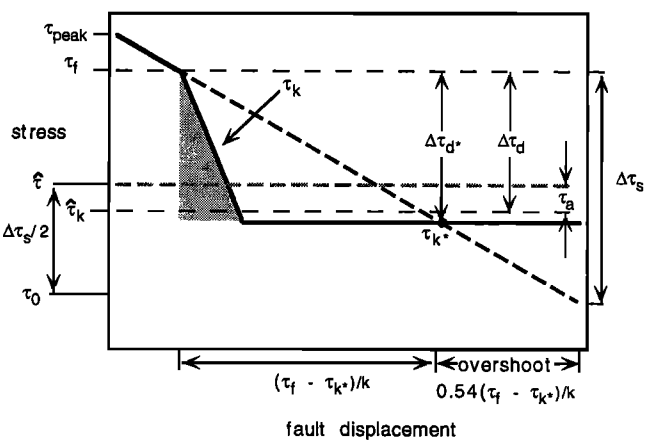

Figure 1. Schematic diagram showing stress (heavy black dashed line) and strength τ_k (heavy black line) as a function of fault displacement during stress drop. The fracture energy (stippled area) and apparent stress τ_a are nonzero, and the dynamic overshoot $\zeta = 0.54$ (see Section 2).

Paper number 2000JB900242.
0148-0227/01/2000JB900242$09.00

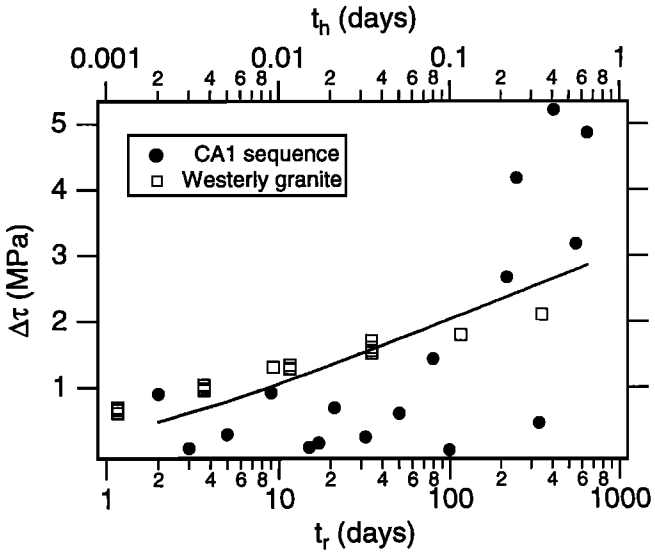

Figure 2. Inferred increases in stress drop with recurrence interval (bottom axis) for small repeating earthquakes on the Calaveras fault, California, calculated from relative moment and rupture duration [CA1, *Vidale et al.*, 1994]. Data for relative moment from Table 1 of *Vidale et al.* [1994] were converted to seismic moment M_o assuming a mean event magnitude M of 1.5 for the 18 events and using the relationship $M_o=10^{1.5M+16}$ [*Hanks and Kanamori*, 1979], where M_o has units of dyne centimeters. The static stress drop was then determined assuming a circular rupture using $\Delta\tau_s = 7M_o/16r^3$ [*Keilis-Borok*, 1959; *Eshelby*, 1957], where radius was calculated from the measured event duration $t_d=r/V_r$, with a constant rupture velocity V_r=1.5 km/s. The line is a least squares fit to the data using the relationship $\Delta\tau=\beta\log(t_r+1)$, which yields β=1.0 MPa. As noted by *Marone* [1998a], the rate of stress drop increase at large t_r is noticeably larger than at short t_r. Shown for comparison is the change in failure strength with hold time t_h (top axis) from slide-hold-slide tests on Westerly granite at σ_e=25 MPa from *Beeler et al.* [1994], after *Dieterich* [1972]. For this laboratory data set $\beta=0.58=2.302b\sigma_e$ and b=0.01. Note the different scales used for t_h and t_r.

range from 1 to 6 MPa/decade, with an average rate of 3 MPa/decade.

In qualitative agreement with the seismic observations, variations in failure strength with recurrence interval are expected on the basis of laboratory observations [*Kanamori and Allen*, 1986; *Scholz et al.*, 1986]. For example, during sliding between initially bare surfaces of quartzofeldspathic rock, the steady-state ratio of shear stress to normal stress, i.e., the frictional strength μ_{ss}, varies with sliding velocity V as $d\mu_{ss}/d\log V=2.30259(a-b)$ [*Ruina*, 1983]. Here, the empirical parameter a-b is the steady-state rate dependence of strength ($d\mu_{ss}/d\ln V$, see equation 6 below) which is approximately constant and less than zero [*Ruina*, 1983]. Assuming that failure strength varies with loading rate in the same way the steady-state strength varies with sliding rate, and that there is an approximately inverse proportionality between recurrence time and loading velocity [*Scholz*, 1990], failure strength μ_f would vary with recurrence time as $d\mu/d\log t_r=2.30259(b-a)$. As pointed out by *Marone* [1998a, 1998b], dimensionless frictional strength drops inferred from experiments should be compared with the seismic observations using dimensioned stress units; thus, because resisting shear stress τ is related to the effective normal stress σ_e by $\tau=\mu\sigma_e$, the implied scaling of failure strength is $d\tau_f/d\log t_r=2.30259(b-a)\sigma_e$. To estimate the variation of stress drop with recurrence, we assume that residual stress is independent of recurrence interval and use typical frictional properties of bare granite; a-b=-0.002 [*Dieterich*, 1986] and μ=0.7 [*Byerlee*, 1978]. If the vertical gradient in the effective normal stress is 18 MPa/km, then $\Delta\tau_s$ will increase with recurrence interval at a rate of 0.4-1.24 MPa/decade at depths of 5-15 km. This rate of increase is somewhat lower than the rate inferred from seismological observations.

More recently *Marone et al.* [1995] and *Marone* [1998a, 1998b] argued that the rate of fault strengthening as observed in laboratory slide-hold-slide tests, rather than the steady-state rate dependence from velocity-stepping experiments, should be employed in laboratory-based estimates of strength recovery. This approach implicitly assumes that a laboratory slide-hold-slide test [*Dieterich*, 1972] represents an analogue of the earthquake cycle, in other words, that the duration of a hold test is analogous to the recurrence interval. In such a test the fault surface slides initially at a steady-state velocity and then the loading velocity is set to zero, during which time the sliding surfaces are held in a condition approaching stationary contact. After some length of time t_h, the hold time, the fault is reloaded by resetting the loading velocity to its original value. Shear stress increases, reaches a peak τ_{peak}, and subsequently returns to its previous steady-state value. The amount of strengthening that occurs during the hold period is given by the difference between τ_{peak} and the steady-state strength. *Dieterich* [1972] found $\mu_{peak}=\tau_{peak}\sigma_e$ to increase linearly with $\ln t_h$, according to $d\tau_{peak}/d\log t_h=2.30259b\sigma_e$ (Figure 2). To estimate the variation of stress drop with recurrence following *Marone* [1998a, 1998b], we again assume that the residual stress is independent of recurrence, equate the hold time t_h with earthquake recurrence interval t_r, and equate τ_{peak} with the failure strength τ_f. Using an effective normal stress gradient of 18 MPa/km and a typical value of b=0.01 from slide-hold-slide experiments on granite at room temperature [*Dieterich*, 1978, 1979, 1986], suggests that $\Delta\tau_s$ should increase with recurrence interval at a rate of 2.1-6.2 MPa/decade at depths of 5-15 km, which is in good agreement with the seismic observations.

However, no direct comparison has been made between scaling of earthquake stress drop with recurrence and that observed in the laboratory during stick-slip sliding; stick-slip, where constant loading leads to periodic or quasi-periodic stress drop, is generally considered to be the laboratory equivalent of repeating earthquake cycles [*Brace and Byerlee*, 1966]. Unfortunately, as discussed above, in previous comparisons between inferred seismic and laboratory stress drops, the earthquake failure stress has been assumed to scale with recurrence interval as inferred indirectly from laboratory tests, e.g., in the same way that steady-state sliding strength scales with sliding velocity in rate-stepping tests [*Scholz*, 1990], (recurrence assumed inversely proportional to loading velocity) or in the same way that strength scales with hold time in slide-hold-slide tests [*Marone* 1998a, 1998b]. Furthermore, to relate seismic stress drop to failure strength, either the residual stress following stress drop or the resistance during stress drop [*Marone et al.*, 1995] is assumed to be independent of recurrence time. Finally, previous laboratory-based predictions of static stress drop for natural earthquakes have tacitly assumed that radiated seismic energy plays no role in determining stress drop size. Thus a comprehensive and self-consistent comparison between

laboratory predictions and seismic observations of strength recovery is warranted.

In this study we compare seismic and laboratory-predicted stress drops by using small event repeating earthquake sequences [*Vidale et al.*, 1994; *Ellsworth*, 1995; *Marone et al.*, 1995; *Nadeau and Johnson*, 1998; *Schaff et al.*, 1999] as the natural counterpart to laboratory stick-slip cycles. We employ a spring-slider model, analogous to the patch model of *Dieterich* [1986], to determine relationships between stress drop, recurrence, and loading velocity that are consistent with the laboratory observations of strength. The spring-slider model, which has been previously found appropriate for earthquake nucleation, is also appropriate for representing dynamic slip and arrest of repeating sequences under restrictive circumstances (discussed below), which we assume apply for the small repeating events considered here. With our spring and slider block model we consider three fault constitutive relations of increasing complexity. First, we use a simple static and kinetic strength relationship which allows us to solve the equations of block motion analytically; this illustrates the general partitioning of energy during dynamic slip and the principal relationship between loading velocity and recurrence interval. Second, we use a time-dependent static/kinetic strength relation to examine the influence of fault strengthening on the relationships between stress drop and recurrence interval or loading velocity. We also use these two static/kinetic strength relations with seismic observations of earthquake recurrence time and geodetic estimates of strain rate to determine the general expected relationship between loading velocity and recurrence interval. Third, we use a rate and state-variable constitutive equation which most fully describes the stick-slip behavior of laboratory faults and which yields different scaling relationships than obtained from the preceding, time-dependent relation.

A major limitation of the spring-slider model is that it predicts a dynamic overshoot that is significantly higher than in continuum models and higher than expected for earthquakes [*Rice and Tse*, 1986]. Since the static stress drop includes contribution from overshoot, static stress drops inferred from this spring-slider model should not be directly compared with seismological values unless differences between the energy budget of the model and that of earthquakes are accounted for. Thus, by estimating the dynamic overshoot from laboratory observations, we propose a scaling relation between static stress drop and recurrence interval for rate- and state-dependent fault strength and compare its predictions against the seismological observations of *Nadeau and McEvilly* [1999] and those compiled by *Marone* [1998a, 1998b].

2. Spring-Slider Block Model and Fault Strength

Failure during small repeating earthquake sequences apparently occurs on an isolated asperity or fault patch embedded in an otherwise aseismically creeping fault zone [*Vidale et al.*, 1994; *Marone et al.*, 1995; *Ellsworth*, 1995; *Nadeau and Johnson*, 1998; *Nadeau and McEvilly*, 1999] (Figure 3a). This geometry is similar to the fixed-length fault patch model described by *Dieterich* [1986], wherein earthquake nucleation on the patch is approximated mathematically by a single degree of freedom spring and slider block (Figure 3b). As follows from *Rice and Tse* [1986], *Boatwright and Cocco* [1996], and others, this type of model can also approximate earthquake dynamic slip and arrest under some restrictive circumstances: (1) the rupture propagates as a classic expanding crack, (2) rupture propagation is stopped by a barrier (e.g., a strong or strongly velocity strengthening region), (3) the material properties of the rupture surface are homogeneous, and (4) stress on the patch is homogeneous or can be well characterized by a spatial average. If criteria (1) and (2) are satisfied, then the duration of slip at a point on the rupture surface is the time it takes the rupture to propagate from that point to the barrier plus the time it takes stress to propagate back to that point from the stopped edge of the rupture. The duration of slip is determined by the wave speed, the rupture velocity, and the rupture dimension and is analogous to the period of the spring and slider block oscillation [*Rice and Tse*, 1986].

For a single degree of freedom spring-slider block, the equation of motion describes the balance between the mass times acceleration and the difference between the spring force $k(\delta_L-\delta)$, (which we have expressed as having units of stress) and the resisting strength τ;

$$\left(\frac{T}{2\pi}\right)^2 \frac{d^2\delta}{dt^2} = (\delta_L - \delta) - \frac{\tau}{k}. \quad (1)$$

Here $T=2\pi\sqrt{m/k}$ is the vibration period of the frictionless system, m is mass per unit area, δ is slip on the fault, δ_L is load point displacement, k is the stiffness of the spring (with units stress/displacement), and the fault strength τ is given by a constitutive relation. Consider a fault that is loaded by the elastic spring at a constant velocity V_L which responds by stick-slip sliding, resulting in stress drops that recur over a time interval t_r. Provided there is no slip during the "stick" phase, the spring accumulates a displacement of $\delta_L=V_L t_r$, corresponding to an elastic stress surplus of $k\delta_L=kV_L t_r$. This surplus is released

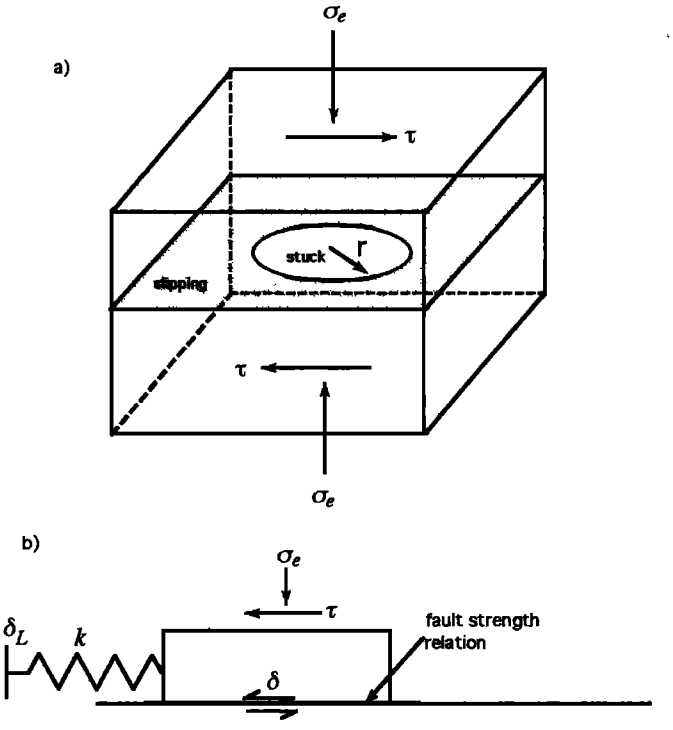

Figure 3. (a) Fault geometry assumed in our analysis of small repeating earthquakes, in which a seismogenic (stuck) patch of radius r is surrounded by an aseismically creeping (slipping) fault plane. The shear and normal stress on the fault plane are τ and σ_e, respectively. (b) A spring-and-slider model corresponding to Figure 3a, in which the block is driven by a load point displacement δ_L acting through a spring with stiffness k.

during the dynamic instability (or "slip" phase), resulting in a stress drop that we assume to be analogous to the static stress drop inferred from seismic moment and fault area for natural earthquakes.

To fully characterize stress drops calculated with (1), we use the failure strength τ_f, the displacement-averaged strength $\hat{\tau}_k$ and the residual stress τ_o (Figure 1); the dynamic stress drop $\Delta\tau_d = \tau_f - \hat{\tau}_k$, and the static stress drop is $\Delta\tau_s = \tau_f - \tau_o$. With the spring-slider block model, slip accelerates so long as the spring force exceeds the fault strength (see Figure 3 below). We identify the stress when the fault strength and the spring force are equivalent as τ_{k*} (Figure 1). The maximum sliding velocity occurs when the acceleration in (1) is zero, coincident with τ_{k*}.

Subsequently, during the "dynamic overshoot", the spring force drops below the kinetic fault strength, the fault decelerates and eventually slip ceases at a stress below the fault strength. Overshoot (Figure 1) measures how much the total slip differs from the amount required to drop the stress from τ_f to τ_{k*}. Here, we express overshoot as the fractional overshoot;

$$\zeta = (\tau_{k*} - \tau_o)/(\tau_f - \tau_{k*}). \quad (2)$$

Note that, as defined here, fractional overshoot varies from ζ=1 (complete overshoot) to 0; whereas the definition of overshoot used by *McGarr* [1999] (also see *Savage and Wood* [1971]) varies from 0.5 to 0 and is not linearly related to (2). An additional difference is we have defined overshoot with reference to τ_{k*}, whereas seismological definitions are usually based on $\hat{\tau}_k$ [e.g., *McGarr*, 1999].

We wish ultimately to compare earthquake stress drop to that predicted by (1), using laboratory-based rate- and state-dependent failure equations to specify τ. However, we first examine simple fault slip relations that are based on a threshold failure criterion. We use simple relations initially because the differences between threshold failure and rate and state failure are slight; rate and state effects are second order [*Dieterich* 1978; 1979; *Ruina*, 1983; *Rice and Ruina*, 1983]. Thus simulation with a simple failure model adequately describes relationships between stress drop, recurrence, and loading velocity, and the partitioning of energy during stress drop. Furthermore, rate and state predictions of dynamic slip are not always intuitive because strength depends nonlinearly on time and sliding velocity. We have found that scaling relations for strength recovery for these rate and state equations can be more clearly illustrated in the context of the predictions of simple models where the equations of motion can be solved analytically.

2.1 Static/Kinetic Strength

Combining a failure criterion having single-valued static and kinetic strengths with (1) illustrates the first-order dynamics of the spring-slider system. Loading occurs while the fault is locked, and slip starts when the shear stress reaches the threshold strength τ_f. At the threshold, the fault strength drops abruptly to a steady sliding resistance τ_k:

$$\begin{aligned} \tau &= \tau_f & V &= 0 \\ \tau &= \tau_k & V &> 0 \end{aligned} \quad (3a)$$

For (3a), the dynamic stress drop is $\Delta\tau_d = \tau_f - \tau_k$. (Figure 4a). The analytic solution of (1) and (3a) for slip as a function of time t during stress drop is

$$\delta = \frac{\Delta\tau_d}{k}\left[\sin\left(\frac{2\pi t}{T} - \frac{\pi}{2}\right) + 1\right], \quad (3b)$$

and sliding velocity with displacement is given by

$$V = \frac{2\pi}{T}\left[\frac{2\delta}{k}\Delta\tau_d - \delta^2\right]^{1/2}, \quad (3c)$$

(Figure 4b) [also see *Scholz*, 1990].

For (3), a total slip of $2(\tau_f - \tau_k)/k$ accumulates during the static stress drop of $\Delta\tau_s = 2(\tau_f - \tau_k)$; $\tau_k = \tau_{k*}$; the static stress drop is twice the dynamic stress drop, and overshoot (2) is complete, corresponding to $\Delta\tau_s = (1+\zeta)(\tau_f - \tau_{k*})$, where ζ=1 (Figure 4). The recurrence time is determined by $\Delta\tau_d$ and the stressing rate $\dot{\tau}$ via

$$t_r = \Delta\tau_s / \dot{\tau} = \frac{\Delta\tau_s}{kV_L} = \frac{2\Delta\tau_d}{kV_L}, \quad (3d)$$

where $\dot{\tau}$ is assumed constant during the interseismic period. Thus, by neglecting any time- or rate-dependent changes in fault strength between earthquakes, there is exactly an inverse proportionality between loading velocity and recurrence interval. Although threshold models such as (3) adequately describe the gross dependence of recurrence interval on loading velocity (for a natural example, see Figure 6b, below), (3d) does not allow static stress drop to depend on recurrence interval as observed for some earthquakes, (as discussed above).

2.2 Time-dependent Static/Kinetic Strength

A static/kinetic strength relation more consistent with seismological observations of increasing stress drop with

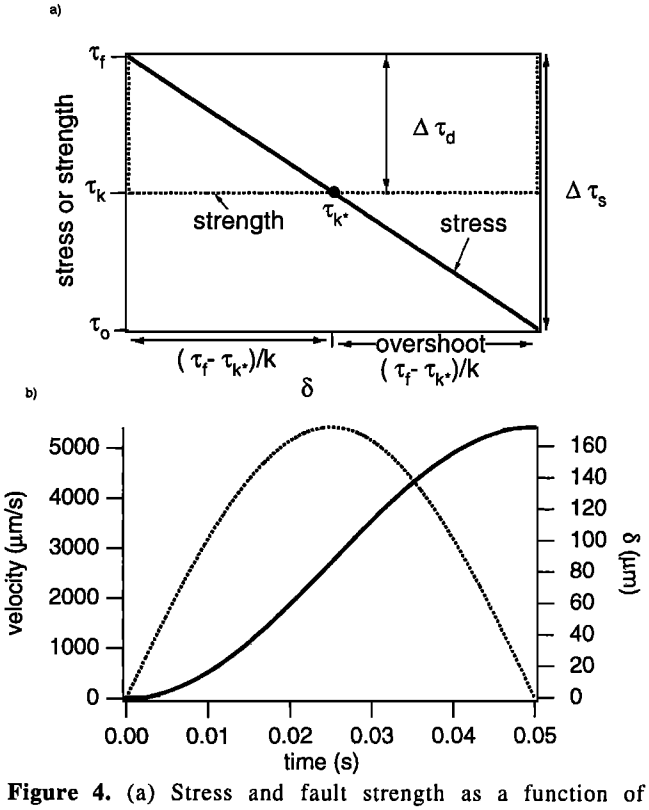

Figure 4. (a) Stress and fault strength as a function of displacement for a simple static/kinetic strength relation, after *Rice and Tse* [1986]. (b) Solutions for slip (solid) (3b) and slip velocity (dashed) (3c) using k=0.0291 MPa/μm, τ_f=15.5 MPa, τ_k=13.0 MPa, and T=0.1 s. These are values representative of the frictional strength of bare quartzofeldspathic faults at room temperature and modest normal stress during stick-slip; e.g., shear strength at failure is $\tau_f = \mu_f\sigma_e$, with μ_f=0.73 and σ_e=21.2 MPa. The choice of T=0.1 s is arbitrary. The value of k used is representative of the stiffness of laboratory testing equipment.

recurrence is one that allows the failure strength to increase with the duration of the interseismic period [*Marone*, 1998a, 1998b]. For purposes of discussion, we choose a form of time-dependent strengthening that is consistent with room temperature slide-hold-slide experiments [*Dieterich*, 1972; *Beeler et al.*, 1994]

$$\tau = \tau_k + B\ln\left(\frac{t}{t_*}+1\right) \quad V=0, \qquad \tau = \tau_k \quad V>0 \tag{4a}$$

where B and t_* are positive constants [*Dieterich*, 1972]. During the interseismic period the fault is locked, and failure occurs at time $t=t_r$ when stress rises to the level of the fault strength. As in Section 2.1, equations (3b) and (3c) specify slip and velocity during stress drop for (4a), except that the dynamic stress drop is now given by $\Delta\tau_d = B\ln(t_r/t_* + 1)$. This time-dependent system (1) and (4a) also requires the static stress drop to be twice the dynamic stress drop ($\zeta = 1$), such that

$$\Delta\tau_s = 2\Delta\tau_d = 2B\ln(t_r/t_* + 1). \tag{4b}$$

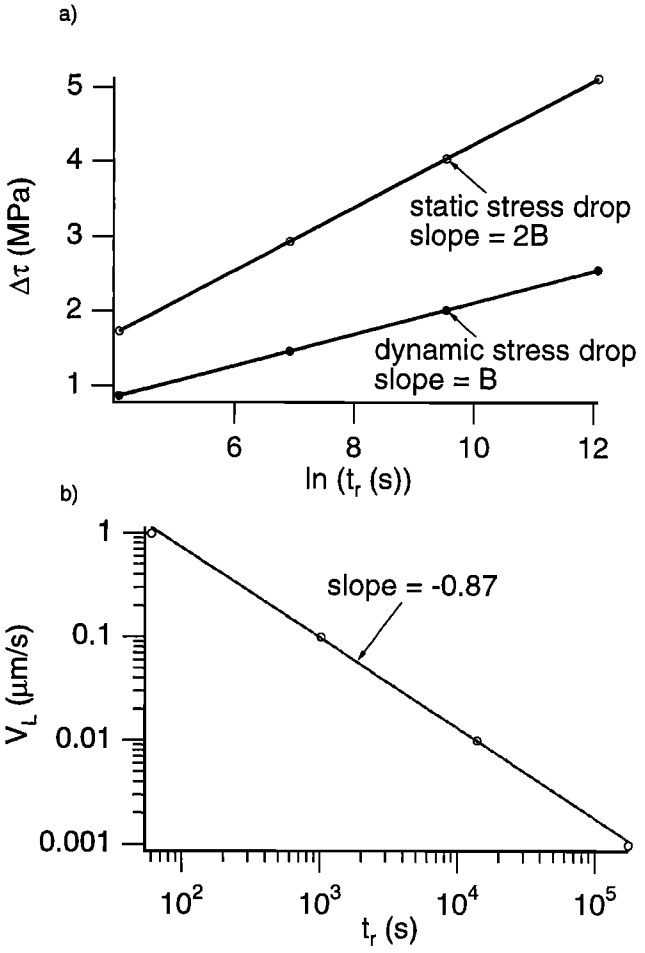

Figure 5. (a) Dynamic and static stress drops versus recurrence time for the time-dependent static/kinetic strength (4), using equation (4b) and the same parameter values used in Figure 4b, with t_*=1.0 s, and B=0.212 MPa. This choice of B reflects a typical value of the rate of time dependent strengthening [*Marone*, 1998a, 1998b] of granite observed at room temperature; e.g., $B=\sigma_e b$ where b=0.01 [*Beeler et al.*, 1994]. (b) Loading velocity versus recurrence interval for the case shown in Figure 5a, calculated from (4c).

The dynamic stress drop given by (4b) has the properties attributed to repeating earthquake sequences by *Marone et al.* [1995] and *Marone* [1998a, 1998b]; namely that stress drop scales linearly with log recurrence time (Figure 5a). Substituting (4b) into $t_r = \Delta\tau_s/kV_L$, we arrive at a relationship between loading velocity and recurrence

$$V_L = \frac{2B}{k}\frac{\ln(t_r/t_* + 1)}{t_r}. \tag{4c}$$

The relationships between V_L and t_r predicted by (3d) or (4c) during stick-slip sliding can be adequately represented by a power law

$$V_L = C\,t_r^{\,n}, \tag{5}$$

where C is a constant. Equation (5) is a general result proposed by *Beeler et al.* [1998] which has subsequently been used to analyze laboratory data [*Karner and Marone*, 2000] and which also can be applied to observational data (as shown below). If there is no slip on the eventual rupture patch during the interseismic period, patch area is constant, and static stress drop is independent of recurrence interval (no time-dependent strengthening), then $C=\Delta\tau_r/k$, n=-1 and the loading velocity is inversely proportional to the recurrence time (3d). However, if time-dependent strengthening causes the failure strength to increase with increasing recurrence time (or with decreasing loading velocity) then n is expected to be >-1 as is well illustrated by the results from (4c) (Figure 5b); the exponent n=-0.87 is somewhat larger than -1.

For earthquakes, while the recurrence time can be measured directly, the loading velocity in a given tectonic setting is usually inferred and subject to interpretation. Loading velocity for large earthquakes, such as those compiled by *Kanamori and Allen* [1986], can be determined more-or-less directly from long-term geodetic or geologic observations, and may vary significantly between inter-plate and intra-plate settings [*Cao and Aki*, 1986; *Scholz et al.*, 1986]. In contrast, loading of the patches responsible for recurring small earthquakes on creeping fault segments in the San Andreas system is arguably controlled by aseismic creep of the fault surrounding each patch [*Ellsworth*, 1995; *Vidale et al.*, 1994], making it more difficult to estimate loading velocities for these events.

Loading rates and recurrence intervals for the CA1 earthquake sequence can be used to test the validity of the proposed general relation (5) for repeating earthquakes. Aseismic creep of the Calaveras fault in the vicinity of the CA1 repeating earthquake sequence is strongly influenced by stress transfer from the 1984 Morgan Hill earthquake (M=6), and the time varying moment release of the CA1 earthquake sequence tracks the overall variation in aseismic strain rate of the fault [*Ellsworth*, 1995]. The loading velocities for the individual CA1 events can be estimated by attributing measured changes in length of the Hamilton to Llagas geodetic line, which crosses the fault obliquely [*Prescott et al.*, 1986; *Marone et al.*, 1995], entirely to aseismic slip of the fault (Figure 6a). As expected from (5), the rate of change of line length shows an approximately inverse correlation with the recurrence time, with an exponent n=-1.2 (Figure 6b). Since the exponent n=-1 is expected if stress drop is independent of recurrence interval (3d), the CA1 sequence appears to confirm that to first-order, seismic faults can be represented by a static/kinetic failure relation. Unfortunately, a more refined analysis necessary to resolve time-dependent effects, and to confirm our assumption that all deformation

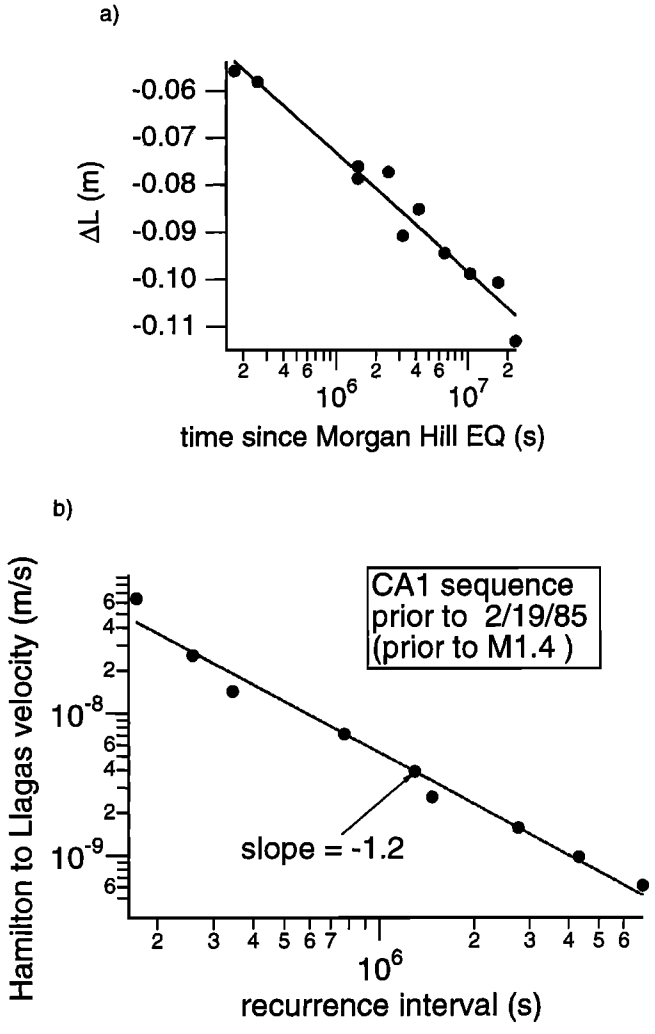

Figure 6. (a) Hamilton to Llagas geodetic line length change for the time period of the CA1 earthquake sequence [*Prescott et al.*, 1986] for events subsequent to the M=6.0 Morgan Hill mainshock on April 24, 1984, and prior to occurrence of a nearby M1.4 earthquake on February 19, 1985. The M1.4 event occurred at a distance of 85 m from the CA1 source region, apparently inducing a significant static stress on CA1 [*Ellsworth*, 1995]. (b) Velocity of the Hamilton to Llagas geodetic line versus recurrence interval for the CA1 sequence events subsequent to the Morgan Hill mainshock and prior to occurrence of the nearby M1.4 event. Velocities were calculated from the straight line fit shown in Figure 6a. As the events in this time sequence are aftershocks of the Morgan Hill mainshock, they are likely induced by accelerated creep (afterslip) on the surrounding fault plane due to the static stress increase imposed by the mainshock.

measured at the surface results from subsurface fault slip, would require more extensive geodetic data.

2.3 Rate- and State-Dependent Strength

Detailed laboratory observations of fault strength differ from the time-dependent (4) and simple static and kinetic strength (3) in two fundamental ways: (1) fault strength depends on sliding velocity and (2) during stick-slip sliding, precursory slip occurs prior to the stress drop. At constant effective normal stress, such behavior is well represented by

$$\tau = \sigma_e \mu = \sigma_e \left(\mu_o + a \ln \frac{V}{V_o} + b \ln \frac{V_o \theta}{d_c} \right) \tag{6a}$$

[*Ruina*, 1983], where θ is a state-variable, which allows strengthening at very low sliding rates and has a steady state value d_c/V. The reference velocity V_o is constant, and d_c is a characteristic displacement associated with changes in shear resistance during sliding. The dependence of the state-variable on time or displacement can be prescribed by one of a number of empirical expressions, which are well described elsewhere [*Ruina*, 1983; *Linker and Dieterich*, 1992]; e.g.,

$$\frac{d\theta}{dt} = -\frac{V\theta}{D_c} \ln \left(\frac{V\theta}{D_c} \right), \tag{6b}$$

or

$$\frac{d\theta}{dt} = 1 - \frac{\theta V}{d_c} \tag{6c}$$

[*Ruina*, 1983]. As predicted by (6) and typically seen during laboratory stick-slip cycles [e.g., *Lockner and Beeler, 1999; Karner and Marone, 2000*], a peak strength is followed by gradual weakening prior to rapid stress drop (Figure 1). Here we distinguish between the peak strength τ_{peak} and the initial stress τ_f; the latter, in this context, is the fault strength at the onset of dynamic slip, and we use "dynamic slip" to indicate that inertial terms are important.

For the purposes of defining stress drop in our numerical calculations (discussed below) we require an unambiguous value of τ_f. *Roy and Marone* [1996] proposed a limiting velocity for quasi-static slip for (6) of $V_{qs} = \sqrt{\sigma_e a d_c / m}$ from which τ_f could be determined using (1) and (6). However, because V_{qs} represents the upper limit of quasi-static slip [*Roy and Marone*, 1996], we choose an arbitrary but intermediate value for the initial stress τ_f, namely the stress corresponding to $V_{qs}/3$. The specific choice of initial stress corresponding to $V_{qs}/3$ or V_{qs} does not affect scaling relationships between stress drop and recurrence because any choice of post-peak initial stress ($\tau_f < \tau_{peak}$ and $V > V_L$) during quasi-static sliding shows the same scaling (see Figure 8 below). We also require a measure of kinetic strength; we use $\mu_{k*} = \sigma_e \tau_{k*}$ the strength associated with the maximum sliding velocity [*Gu and Wong*, 1991] which is useful for relating stress drop to dynamic overshoot for the spring and slider block model (Figure 1). We distinguish between a measure of dynamic stress drop appropriate for the spring and slider block model $\Delta\tau_{d*} = \tau_f - \tau_{k*}$ and the seismological definition $\Delta\tau_d = \tau_f - \hat{\tau}_k$. In these numerical calculations with (6), most of the slip occurs at or near the maximum velocity [*Rice and Tse*, 1986], $\mu_k \approx \mu_{k*}$ ($\mu_{k*}/\mu_k = 0.99$), μ_{k*} well represents the mean strength (see Figure 8a below), and $\Delta\tau_{d*} \approx \Delta\tau_d$.

Fully dynamic calculations with (6) result in different scaling between stress drop and recurrence interval than with (4). For example, numerical simulations by *Gu and Wong* [1991] using (6a) and (6b) over a wide range of constitutive parameters and stiffness show that the static stress drop scales linearly with $2(a-b)\ln V_L$ (Figure 7a). Qualitatively similar results were reported in the earlier study of *Cao and Aki* [1986]. While *Gu and Wong* [1991] did not explicitly address scaling of stress drop with recurrence time, their unpublished data indicate that the relationship between loading velocity and recurrence follows the general power law relationship (5) (Figure 7b). In the example shown in Figure 7, because n in this case is only slightly greater than −1 (n=-0.95), the static stress drop scales approximately by $2(b-a)\ln t_r$ (Figure 7a).

Neither *Gu and Wong* [1991] nor the earlier study of *Cao and Aki* [1986] used a fault strength relation that allows for time-dependent strengthening in the absence of slip that some recent laboratory studies suggest is important [*Beeler et al.*, 1994; *Nakatani and Mochizuki*, 1996]. To incorporate this effect, we have extended the spring-slider simulations of *Gu and Wong* [1991] to consider (6c), which has the desired property that $d\theta/dt$=1 when V=0 [*Linker and Dieterich*, 1992]. Our simulations were conducted using a Runga-Kutta scheme with adaptive step-size control and fifth-order errors [*Press et al.*, 1986]. Stick-slip was induced in the simulations by increasing the load point velocity of a fault sliding initially at steady-state. Following the change in sliding velocity, the first few stick-slip cycles have varying stress drops, but subsequent events are characteristic, with event to event variation in stress drop of < 0.2%. Sequences of 13-15 stick-slip cycles were calculated at five different loading velocities ranging from 0.01–1.0 μm/s; the quantities shown in Figure 8 represent the average of the last three stick-slip cycles at each loading velocity.

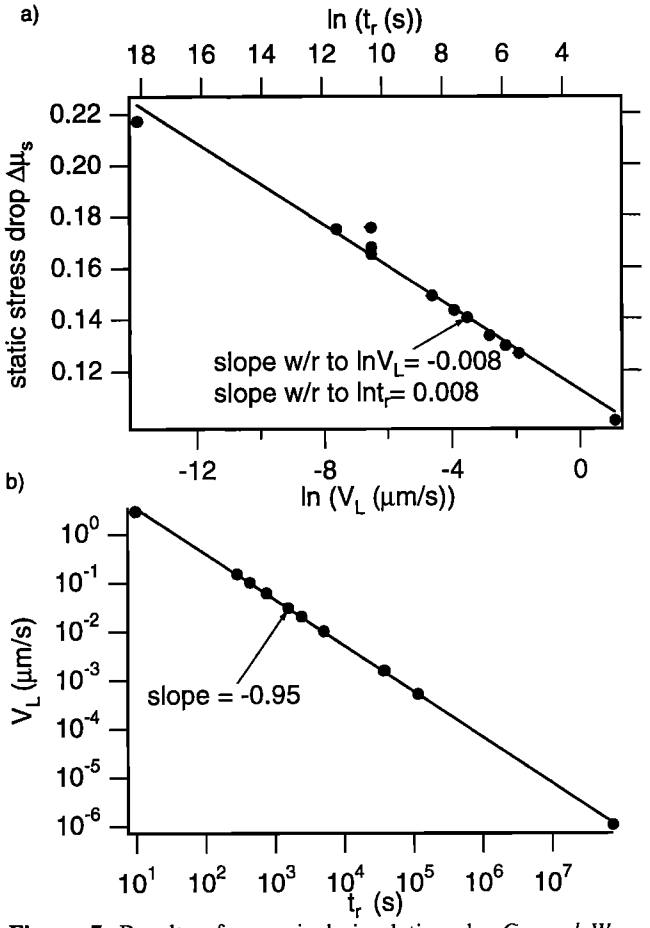

Figure 7. Results of numerical simulations by *Gu and Wong* [1991] using (6a) and (6b). (a) Static stress drop, expressed in terms of a change in the ratio of shear stress to normal stress (black dots), versus both loading velocity and recurrence time. The static stress drop as defined by *Gu and Wong* [1991] is the difference between the peak strength prior to stress drop and the residual stress after rapid slip has ceased. Also shown is a least squares fit of a straight line to these simulations, with slope indicated both with respect to V_L and t_r. Here the original dimensionless simulations, conducted at $(b\text{-}a)/a$=1, were dimensioned using approximate values of the relevant strength parameters from room temperature laboratory experiments [e.g., *Marone*, 1998b]: b=0.008, $b\text{-}a$ =0.004, σ_e=21.2 MPa, d_c=1.0 μm, and V_o=0.001 μm/s. (b) Loading velocity versus recurrence time from these simulations, using previously unpublished data from the *Gu and Wong* [1991] study. The results of the numerical calculations are shown as black dots, with a least squares fit of a straight line.

Results of these simulations using the spring-slider model with equations (1), (6a) and (6c) at the five different loading velocities indicate that dynamic $\Delta\tau_{d*}$ and static stress drops scale with $(a\text{-}b)\ln V_L$ and $2(a\text{-}b)\ln V_L$, respectively (Figure 8a). These simulations also show that μ_{k*} is essentially independent of loading velocity and that peak stress and initial stress decrease with increasing loading velocity in nearly the same way as the dynamic stress drop (Figure 8a). Thus, by our definition of the dynamic stress drop $\Delta\tau_{d*}$, its scaling results entirely from variations in the initial stress. As with the simple models presented in Sections 2.1 and 2.2, for laboratory values of constitutive parameters, rate and state equations both with and without time-dependent strengthening require the static stress drop to be nearly twice the dynamic stress drop (Figures 7a and 8a) corresponding to $\Delta\tau_s \approx (1+\zeta)\Delta\tau_{d*}$, where $\zeta \approx 1$. Finally, comparison of Figures 7a and 8a indicates that, for fault constitutive parameters appropriate for laboratory experiments, the scaling relations between stress drop and either V_L or t_r for the two forms of state evaluated are nearly identical.

The relationship between loading velocity and recurrence time for (6c) (Figure 8b) is similar to the simulations of *Gu and Wong* [1991] (Figure 7b) and, for values of $a\text{-}b$ and d_c consistent with laboratory observations, is predicted by the general power law relationship (5) (n=-0.94) (Figure 8b). In this case, as $n \approx -1$, the dynamic stress drop for (6c) scales approximately as $(b\text{-}a)\ln t_r$, and static stress drop scales approximately as $2(b\text{-}a)\ln t_r$ (Figure 8a). Note that in the case of the static stress drop, the scaling of the simulated value is slightly less than the expected value of $2(b\text{-}a)\ln t_r$ (slope=0.007 as opposed to 0.008). The smaller value reflects smaller dynamic overshoot (see Section 2) for (6c) than (6b), as has been noted by *Ben-Zion and Rice* [1997].

In our simulations, $\hat{\tau}_k \approx \tau_{k*}$; however it is possible with other choices of constitutive parameters for (6) that $\hat{\tau}_k \neq \tau_{k*}$, for example as shown schematically in Figure 1. In this case the "fracture energy" [*Wong*, 1986], the amount of energy expended in dropping the fault strength from τ_f to τ_{k*}, (shaded region in Figure 1) is significant. For significant fracture energy, the stress drop will be smaller than in the cases shown in our study, and the scaling we have calculated (e.g., Figures 7 and 8) is the upper bound. Thus, to summarize our results for both of the rate and state equations considered here (Figures 7a and 8a), we find that variations in stress drop with recurrence time should be bounded by

$$d\Delta\tau_{d*}/d\ln t_r \leq \sigma_e(b-a), \tag{7a}$$

$$d\Delta\tau_d/d\ln t_r \leq \sigma_e(b-a), \tag{7b}$$

and

$$d\Delta\tau_s/d\ln t_r \leq 2\sigma_e(b-a), \tag{7c}$$

where we have converted dimensionless friction to shear stress by multiplying by the effective normal stress [*Marone*, 1998b].

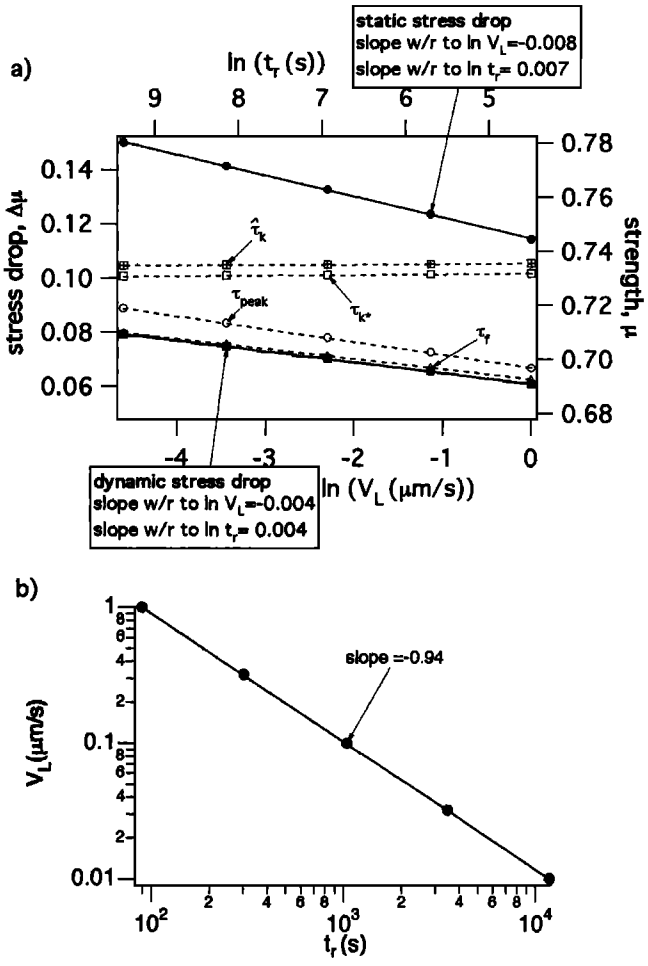

Figure 8. Results of rate and state-variable simulations using (6a) and (6c) with b=0.012, $(b\text{-}a)$=0.004, μ_o=0.7, d_c=1 μm, k=0.0291 MPa/μm, σ_e=21.2, and T=0.1 s. These are approximate parameter values appropriate for the frictional strength of granitic rocks at room temperature during stick-slip at modest normal stress, chosen to match the steady-state rate dependence in the simulations by *Gu and Wong* [1991]. The choice of T=0.1 s is arbitrary. The value of k used is representative of the stiffness of laboratory testing equipment. (a) Static and dynamic stress drop versus both loading velocity and recurrence time (left axis scale). The numerical results of these simulations are shown as solid symbols, with least squares fits of straight lines (solid lines). The slopes of these lines are indicated both with respect to V_L and t_r. The static stress drop $\Delta\tau_s$ is the difference between the stress at the onset of dynamic motion τ_f and the residual stress τ_o, while the dynamic stress drop $\Delta\tau_{d*}$ is the difference between stress at the onset of dynamic motion τ_f and the strength at the maximum sliding velocity τ_{k*} (see text). Also shown as open symbols are the peak stress τ_{peak}, the initial stress prior to dynamic slip τ_f, the mean shear stress $\hat{\tau}_k$, and the dynamic strength at the maximum sliding velocity τ_{k*}, with least squares fits (dashed lines) (right axis scale). The dynamic strength at the maximum sliding velocity and the mean shear stress have been shifted vertically by 0.1. (b) Loading velocity versus recurrence time for the same simulations shown in Figure 8a.

3. Discussion

3.1. Dynamic Stress Drop

As pointed out above, the scaling of dynamic stress drop with recurrence time in numerical simulations of stick-slip cycles with rate and state-variable strength (6) results because: (1) the value of strength at the onset of dynamic motion scales with $(b\text{-}a)\ln t_r$ and (2) the kinetic fault strength during dynamic slip (the dynamic strength) is independent of recurrence interval or loading velocity (Figure 8a). In the present paper we do not present rigorous mathematical discussion of the numerical results from these simulations; a comprehensive discussion of these and other simulations is included in a forthcoming paper [*T.-f. Wong et al.*, manuscript in preparation, 2001]. However, the $(b\text{-}a)$ scaling of dynamic stress drop with recurrence time can be rationalized in fairly simple terms by considering contributions of rate and state effects both to the peak strength and to the dynamic strength. Here we use the peak strength as a proxy for the strength at the onset of dynamic slip because they show the same scaling (Figure 8) and because the sliding velocity at the peak is well defined (see below).

We first consider peak strength scaling. For true time-dependent strengthening (6c), the evolving state-variable term contributes to changes in peak strength as $b\ln t_r$ [*Dieterich*, 1972; *Beeler et al.*, 1994; *Marone*, 1998a, 1998b]. Noting that the equation of motion appropriate for quasi-static sliding ($d\mu/dt=k(V_L\text{-}V)$) requires that $V=V_L$ at the peak shear stress, we find that the contribution to peak strength from the direct velocity dependence of friction is $a\ln V_L$. Since $V_L \propto t_r^n$, where $n\approx$-1 (Figures 7b and 8b), the corresponding contribution of the direct rate dependence to peak strength is roughly $-a\ln t_r$. Adding the contributions from the state-variable and the direct rate dependence indicates that peak stress should scale linearly with $(b\text{-}a)\ln t_r$. However, this scaling argument cannot be applied to the state-variable relationship (6b) studied by *Gu and Wong* [1991] because their state variable is not truly time dependent. A more general but non-rigorous way to rationalize the $(b\text{-}a)$ scaling between peak strength and recurrence time is obtained by using the substitution $b\ln V_o\theta/D_c = b\ln V_o/V + b\ln V\theta/D_c$ and rewriting (6a) in the form

$$\mu = \mu_0 + (a-b)\ln\frac{V}{V_0} + b\ln\frac{V\theta}{D_c}. \qquad (8)$$

Again, noting that $V=V_L$ at peak strength, the difference between peak strengths at different loading velocities is

$$\Delta\mu_{peak} = (a-b)\ln\frac{V_2}{V_1} + b\ln\frac{V_2\theta_2}{V_1\theta_1}. \qquad (9)$$

If, as expected, $\theta \propto t_r$ at peak strength [*Marone*, 1998a; 1998b], and $V_L \propto t_r^n$ with $n\approx$-1 (Figures 7b and 8b), then the state-variable θ at peak strength scales inversely with velocity $V=V_L$. In this case, the ratio of $V_1\theta_1 / V_2\theta_2$ is close to 1 and the second term on the right-hand side of (9) is approximately zero, resulting in $\Delta\mu_{peak} \approx (b-a)\ln V_1/V_2$. Again, accounting for the observed relationship between loading velocity and recurrence (Figure 7a) yields $\Delta\mu_{peak} \approx (b-a)\Delta\ln t_r$.

Constancy of the dynamic strength with loading rate is the other key to understanding the scaling of dynamic stress drop with recurrence for rate and state-variable equations. The insensitivity of dynamic strength to loading velocity results from: (1) a weak dependence of dynamic strength on sliding velocity and (2) a weak dependence of available energy for stress drop on loading velocity. Although sliding velocity varies significantly, the particular values of fault strength and sliding velocity during dynamic stress drop correspond to steady-state values [*Rice and Tse*, 1986]. Thus, since for (6a) $d\mu_{ss}/d\ln V=(a\text{-}b)$ and $a\text{-}b$ is typically very small (in this case, -0.004), dynamic strength should depend only weakly on the sliding velocity. The average sliding velocity during stress drop is determined by this weak

dependence of strength on sliding rate and by the amount of potential energy available to drive slip. The potential energy available to drive fault slip scales with τ_f (alternatively, with the peak stress) which, as discussed above, varies weakly with loading velocity ($d\mu/d\ln V=(a-b)$). Thus, the average sliding velocity during stress drop will vary weakly with loading velocity, and the kinetic strength will vary extremely weakly with loading velocity.

3.2. Scaling of Slide-Hold-Slide Peak Strengths

The scaling of peak strength with hold time from conventional slide-hold-slide tests (Figure 2) is not the same as the scaling of peak strength with recurrence obtained from stick-slip cycles (Figures 7 and 8) because the contribution from the direct rate dependent term $a\ln V$ in (6a) is different in each case; for stick-slip, different peak strengths correspond to different slip rates ($V=V_L$ at peak), while the peak strengths from hold tests, regardless of duration, generally correspond to the same slip velocity. Hold test results do, however, provide an alternative way of understanding the tradeoffs between time-dependent strengthening represented by the state-variable θ and weakening due to the direct velocity dependence of the $a\ln V$ term in (6a). For example, sets of slide-hold-slide tests in which reloading rate was held constant during a given set but varied between sets [*Kato et al.*, 1992; *Marone*, 1998a] confirm that the peak strength not only depends on hold duration but also on the loading rate, as expected from (6) and the requirement that $V=V_L$ at peak stress.

One can conduct laboratory experiments in which hold time and reloading velocity are systematically varied so as to independently investigate the dependence of μ on V as well as on hold time. In particular, using (6a) and (6c), the constitutive parameter a might be extracted by comparing a set of hold tests of different hold duration with a similar set reloaded at a different velocity; $(b-a)$ might also be extracted in this way, provided that variations in reloading velocity and hold duration are synchronized (as described below). To illustrate this approach, we first conducted numerical simulations of conventional slide-hold-slide tests using a starting sliding velocity of V=0.1 μm/s. Following hold periods of 3.16, 10, 31.6, 100, 316, 1000, 3162, and 10000 s, the fault was reloaded at a velocity equal to the starting velocity. We then conducted three more sets of slide-hold-slide simulations using the same eight hold intervals and starting velocity of V=0.1 μm/s but with each of these three sets reloaded at different velocities of 0.32, 1.0, or 3.16 μm/s (Figure 9). Note that the hold times and reloading velocities are synchronized such that the ratio of successive hold times within a set (e.g., 3.16 s/10 s) equals the ratio of loading velocities employed in successive sets (0.32 μm/s/1.0 μm/s). Each resulting set of peak strengths reloaded at the same velocity shows $b\ln t_h$ scaling at large t_h, as required by (6c) [*Beeler et al.*, 1994]. There is also systematic vertical offset between sets reloaded at different rates, similar to that observed in the experiments of *Marone* [1998a]. This vertical offset in our simulations (Figure 9) should be equal to $a\ln V_1/V_2$, where V_1 and V_2 are the loading velocities for the different hold sets [*T. Tullis*, pers. comm., 1997], provided that θ is approximately constant for holds of the same duration but reloaded at different velocities. We have used a stiffness appropriate for a compliant testing machine; since we find the predicted $a\ln V_1/V_2$ spacing, we conclude that this method of Tullis may be generally useful for measuring a directly with hold tests.

Furthermore, if our particular testing procedure is followed, one can also construct a "strengthening" line that reflects both the natural log time-dependent strengthening and the natural log rate-dependence. The construction is made by choosing an arbitrary peak strength for a particular recurrence interval, e.g., that corresponding to 3162 s in the V_L=3.16 μm/s set, and then selecting values of peak strength at each subsequent hold time on subsequent hold sets corresponding to an incremental change in loading velocity (Figure 9). The difference in peak strength for successive points on the construction is $\Delta\mu=a\ln V_1/V_2+b\ln t_{h1}/t_{h2}$, and since the loading velocities and hold times were chosen so that $V_1/V_2=t_{h2}/t_{h1}$, the slope of the constructed line is $\Delta\mu/\Delta\ln t_h=(b-a)$. This expectation is confirmed by a linear least squares fit (dashed line, Figure 9) with slope $(b-a)$.

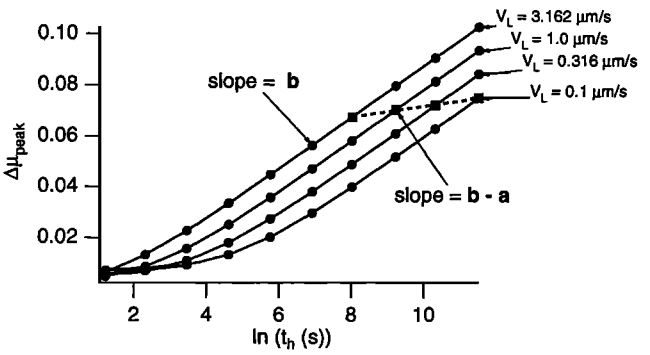

Figure 9. Numerical simulations of peak strength as a function of hold time t_h from suites of slide-hold-slide tests loaded initially at a velocity of 0.1 μm/s but reloaded at the different velocities indicated. Calculations were carried out using (6a), (6c), and $\mu=k(\delta_L-\delta)/\sigma_e$ with b=0.010, $(b-a)$=0.002, μ_o=0.7, d_c=5 μm, and k/σ_e=0.0021 /μm. These are parameter values appropriate for the frictional strength of granitic rocks at room temperature and modest normal stress. The value of k used is representative of the stiffness of laboratory testing equipment. Values for the parameters b and $(b-a)$ might be obtained from actual experiments using this testing procedure by comparing peak strength at variable hold time but constant reloading velocity (solid lines) and by comparing peak strength at variable hold time and variable reloading velocity (dashed line), as indicated.

3.3. Role of the $a\ln V$ Term in Failure

Our numerically calculated stress drops, section 2.3, suggest that $b\ln t_r$ scaling of dynamic stress drop [*Marone et al.*, 1995; *Marone* 1998a, 1998b] is possible if $a<<b$. However, this implies that strength drop is abrupt ((3) or (4), see *Gomberg et al.* [2000]), which is generally not observed. Furthermore, it is very unlikely that any real geologic material would exhibit negligible direct rate dependence ($a\approx 0$) because inelastic deformation in the brittle (or ductile) field invariably shows instantaneous rate strengthening. For example, the failure stress of intact rock shows a positive rate dependence, which is likely due to the subcritical growth and coalescence of microfractures [*Scholz*, 1968a, 1968b; *Lockner*, 1998]. *Lockner* [1998] noted that both the form ($a\ln V$) and the size of the rate dependence of strength for intact Westerly granite is indistinguishable from the instantaneous rate dependence of fault strength as measured during bare-surface and simulated-gouge shearing experiments in Westerly granite. As wear involving fracture is a by-product of slip between bare fault surfaces, and grain fracture results from the shearing of granular gouge layers at high normal stress, it is not surprising that all types of experimental shear deformation in the brittle field show a similar instantaneous rate dependence of strength. Thus, even if the micromechanical details of earthquake nucleation more closely resemble the failure of intact rock than they do stick-slip

on precut rock surfaces, failure stress and therefore the stress drop will have a second-order dependence on the loading rate. On the basis of experimental observations where positive rate dependence is observed at room temperature, ranging from fractures in single crystals [*Atkinson*, 1984] to fault slip [*Dieterich*, 1978] and rock fracture [*Lockner*, 1998], it is reasonable to assume that such behavior is symptomatic of brittle rock deformation at room temperature. Provided that subcritical fracture is also rate dependent at elevated temperature, as is indicated by the experiments of *Atkinson* [1984], and that earthquake failure involves a significant component of fracturing, it is likely that earthquake stress drop will reflect an instantaneous positive rate dependence similar to that observed in low-temperature experiments.

3.4. Static Stress Drop

For values of a-b and d_c consistent with laboratory observations, the spring-slider model (1) and (6) predicts a dynamic overshoot (2) that is nearly complete and significantly higher than expected for earthquakes [*Rice and Tse*, 1986]. Complete dynamic overshoot, as we have defined it (Section 2), occurs when both the fracture energy and the radiated energy are negligible. Since the static stress drop includes contribution from overshoot, static stress drops inferred from this model can not be directly compared with seismological values unless differences in energy between the spring-slider model and earthquakes are accounted for.

For direct comparison with seismic observations, scaling between recurrence and stress drop in spring-slider calculations can be modified to account for radiated energy, not included in (1), and for fracture energy, which is not significant in laboratory friction experiments [*Okubo and Dieterich*, 1984], by reducing the amount of dynamic overshoot. From (2), the stress drop in excess of $\tau_f - \tau_{k^*}$ is given by $\tau_{i^*} - \tau_o = \zeta(\tau_f - \tau_{k^*}) = \zeta\Delta\tau_{d^*}$, so that

$$\Delta\tau_s = (1+\zeta)\Delta\tau_{d^*}. \tag{10}$$

For the case of rate- and state-dependent strength, we combine this result (10) with (7a) and find static stress drop to scale with recurrence as

$$d\Delta\tau_s / d\ln t_r \le \sigma_e(1+\zeta)(b-a). \tag{11}$$

Equation (11) is the principal result of our analysis. In the case of no radiated or fracture energy there is complete overshoot, ζ=1, and we retrieve from (11) the scaling predicted by the spring-slider model (equation 7c). Using the laboratory data of *Lockner and Okubo* [1983], summarized by *McGarr* [1994], we assume negligible fracture energy so that (2) is $\zeta = (\hat{\tau}_i - \tau_o)/(\tau_f - \hat{\tau}_i)$, and find a median of ζ=0.35 and an average of ζ=0.37. For depths of 5-15 km, using an effective normal stress of 18 MPa/km, ζ=0.37, and b-a=0.002 in (11) results in an increase in static stress drop with recurrence of 0.57-1.70 MPa/decade, which is toward the low end of the 1 to 6 MPa/decade range of strengthening rates obtained from seismic observations [*Marone*, 1998a, 1998b]. If fracture energy is larger for earthquakes than in the experiments of *Lockner and Okubo* [1983], or in our laboratory-based simulations, overshoot will be smaller; thus our predicted scaling between recurrence and static stress drop using laboratory-estimated overshoot is an upper bound. We conclude that seismic observations of increased stress drop with recurrence probably cannot be explained by room temperature laboratory observations alone.

3.5. Limitations of the Laboratory and Seismological Observations

To what extent could room temperature laboratory observations of the shear strength of smooth, flat rock surfaces in contact quantitatively explain interseismic strength recovery of non-planar natural fault zones that may occur under hydrothermal conditions? Reasonable geothermal gradients require that the temperatures appropriate for the large crustal earthquakes of *Kanamori and Allen* [1986] are hundreds of degrees higher than in room temperature experiments. Solid state deformation processes thought to be responsible for fault strengthening through increase in contact area in room temperature experiments [*Dieterich*, 1972; *Scholz et al.*, 1972; *Dieterich and Kilgore*, 1994], such as subcritical fracture growth or dislocation activity, are thermally activated. Thus, the rates of these processes at seismogenic depths should be greater than at room temperature, even for the shallow repeating sequences discussed above. In particular, fault slip at hydrothermal conditions using simulated quartz and granite fault gouges confirm that rate dependence does increase with increasing temperature under water-saturated conditions [*Blanpied et al.*, 1995; *Chester*, 1995]. Furthermore, interpretation of geologic observations from exhumed faults and of laboratory experiments conducted at elevated temperatures in the presence of water provide some arguments that interseismic strength recovery might be augmented by chemical fluid-rock interaction processes such as crack healing and hydrothermal alteration [*Power and Tullis*, 1989; *Fredrich and Evans*, 1992; *Hickman and Evans*, 1992, 1995; *Chester et al.*, 1993; *Karner et al.*, 1997; *Olsen et al.*, 1998]. Also, such lithification processes would possibly influence the fracture energy. Therefore, any agreement between room-temperature laboratory and seismological determinations of interseismic strengthening rates may be fortuitous, and more systematic investigations of fault strength under elevated temperatures in the presence of natural chemically reactive fluids are necessary.

In comparing laboratory and field observations, some of the uncertainties associated with the seismological observations should also be kept in mind. In particular, quantitative estimates of the rate of increase in stress drop with recurrence time depend significantly on assumptions made in converting moment to stress drop. For example, for the data shown in Figure 2, relative moments from *Vidale et al.* [1994] were converted to stress drop assuming constant rupture velocity (see caption). This leads to a rate of stress drop increase with recurrence of ~1 MPa/decade which is at the lower limit of the published observations [*Marone*, 1998a, 1998b]. However, rupture duration for individual events within the CA1 sequence also varies systematically with relative moment; so, alternatively, one could assume that rupture area is constant and rupture velocity varies with moment for these events [*Marone et al.*, 1995]. The same relative moment data of *Vidale et al.* [1994] has been used to justify rates as high as 6 MPa/decade [*Marone*, 1998a], which falls at the upper limit of published interseismic strengthening rates [*Marone* 1998a, 1998b]. Moreover, for some repeated sequences, seismic moment decreases with recurrence [e.g., the CA2 sequence, *Marone et al.*, 1995], which cannot easily be explained by interseismic restrengthening.

Much smaller uncertainties in the variation of seismic moment with recurrence are found for repeating sequences along the San Andreas fault at Parkfield, where preliminary results indicate moment increases by ~18%/decade, with a formal uncertainty of 3.5%/decade [*Nadeau and McEvilly*, 1999]. Although these

results are consistent with the largest strengthening rates we infer from fault slip in room-temperature experiments (e.g., 1.7 MPa/decade, using (11) with a 10 MPa stress drop is a 17%/decade change), there are complications. By assuming that all the plate motion is relieved seismically, *Nadeau and Johnson* [1998] conclude that the stress drops for these small events are extremely high, having typical values of $\Delta\tau_r$=1000 MPa. Although highly model-dependent, if these stress drops are correct, then the required rate of interseismic restrengthening would be 180 MPa/decade, a rate roughly 2 orders of magnitude higher than the laboratory observations. Thus, in a case where the uncertainty in seismic moments is small, the laboratory-inferred rates of strengthening could be considerably smaller than for natural faults. However, the inferred high stress drops for the Parkfield sequences are controversial, and if only a portion the surface-measured fault motion is relieved seismically at the source of the repeating events, the stress drops could be typical (e.g., 10 MPa) [*Anooshehpoor and Brune*, 2001; *Sammis and Rice*, 2001].

All of our conclusions about static stress drop scaling with recurrence are based on assumptions of homogeneous material properties, crack-like stress distributions, and crack-like rupture propagation and rupture arrest. Our analysis of static stress drop scaling will not apply if ruptures arrest at points in the interior of the ruptured region due to local geometric effects (abrupt locking [*Brune*, 1970]) or local variations in fault strength (a self-healing slip pulse [*Heaton*, 1990]). In these cases, dynamic stress drop can exceed the static stress drop (undershoot), a situation that is not possible with conventional spring-slider models. However, to date, there is no indication that undershoot occurs during small repeating earthquake sequences.

It is also difficult to confidently extrapolate our results from the small repeating events to larger, more hazardous earthquakes. Our assumptions of homogeneous material properties and crack-like stress distribution, while perhaps plausible for small earthquakes, are probably not appropriate for large events, which are more likely to have variable material properties and heterogeneous distributions of pre-stress [*McGarr and Fletcher*, 2001]. In addition, since large events have much larger coseismic slip, shear heating effects such as transient pressurization or melting should influence the kinetic strength [*Sibson*, 1973; *Lachenbruch*, 1980]. In assigning laboratory-like fault strengths to natural faults, we assume an effectively constant kinetic strength, whereas for a shear melted or partially melted material the sliding resistance might be a significant function of the slip velocity. In this case, the manner in which stress drop scales with recurrence interval might be significantly different than obtained in our modeling study.

All of our conclusions about scaling of stress drop with loading velocity and recurrence are derived from a series of simulations, each at constant loading velocity. It may be reasonable to assume, as we implicitly argue, that similar variations in stress drop with recurrence should result if the loading velocity is time varying, e.g., as shown in Figure 6b for the CA1 sequence of *Vidale et al.* [1994]. However, note that complex behavior can arise with rate and state formulations, even at constant loading rate, particularly when (6c) is used [*Rice and Ben-Zion*, 1996]. Thus, some caution should be undertaken in applying the scaling relationship (11). An additional limitation to (11) is that it applies only at "long" recurrence time, in that the logarithmic dependence implies an infinite increase in stress drop from t_r=0 to some measurable recurrence time t_r>0 [*M. Nakatani*, pers. comm., 2000]. Ideally, the validity and limits of (11) will be established by subsequent experiments and field observations.

4. Conclusions

During the earthquake cycle, fault loading velocity V_L is related approximately to recurrence interval t_r by a power law $V_L \propto t_r^n$; the power law exponent can be used to distinguish apparent time-dependent strengthening (n>-1) from weakening (n<-1). Deviations from n=-1 arise due to deviations of fault failure strength from a threshold value, e.g., from rate- or time-dependent effects on fault strength. These deviations are expected to be small based on room-temperature laboratory observations of fault strength. For laboratory-based constitutive equations, dynamic stress drop scales linearly with log recurrence interval according to $(b-a)\ln t_r$. General consideration of brittle deformation suggests that stress drop in the Earth will scale in a way similar to the laboratory results. In particular, increases in stress drop with recurrence due to time-dependent strengthening, represented in laboratory-based constitutive equations by the coefficient b, will be counteracted by a positive rate dependence of failure strength represented by the coefficient a. Failure strength is expected to have a positive rate-dependent component in any instance where deformation involves some component of subcritical fracture growth. We conclude that if natural fault strength is controlled by the same physical processes responsible for room-temperature laboratory-observed fault strength, then variations of static stress drop with recurrence should satisfy the relation $d\Delta\tau_s/d\ln t_r \le \sigma_e(1+\zeta)(b-a)$, where σ_e is effective normal stress and ζ is the fractional overshoot. Seismic observations of stress drop increasing with recurrence interval probably cannot be explained by room temperature laboratory observations alone. However the discrepancy between room temperature experiments and the seismic observations is less than an order of magnitude.

Acknowledgments. Research at Stony Brook was partially supported by the National Science Foundation under grant EAR9805072. This article was greatly improved due to comments or discussions with G. Beroza, D. Schaff, B. Ellsworth, A. McGarr, C. Marone, T. Tullis, and, in particular, M. Nakatani and the associate editor T. Yamashita. NMB is grateful to T. Tullis and J. Weeks for a number of lengthy discussions of fault zone energy. Thanks also to C. He, J. Boatwright, and B. Nadeau for providing their unpublished data, to David Schaff for providing the geodetic data, and to T. Tullis for sharing his unpublished ideas and computing facilities.

References

Anooshelpoor, A., and J. N. Brune, Quasi-static slip-rate shielding by locked and creeping zones as an explanation for small repeating earthquakes at Parkfield, *Bull. Seismol. Soc. Am.*, 91, 401-403, 2001.

Atkinson, B. K., Subcritical crack growth in geologic materials, *J. Geophys. Res.*, *89*, 4077-4114, 1984.

Beeler, N. M., T. E. Tullis, and J. D. Weeks, The roles of time and displacement in the evolution effect in rock friction, *Geophys. Res. Lett.*, *21*, 1986-1990, 1994.

Beeler, N. M.. T.-f. Wong, and S. H. Hickman, Stress drop and interseismic strength recovery, *Eos, Trans., Am. Geophys. Un.*, *79*, 224, 1998.

Ben-Zion, Y., and J. R. Rice, Dynamic simulations of slip on a smooth fault, *J. Geophys. Res.*, *102*, 17,771-17,784, 1997.

Blanpied, M. L., D. A. Lockner, and J. D. Byerlee, Frictional slip of granite at hydrothermal conditions, *J. Geophys. Res.*, *100*, 13,045-13,064, 1995.

Boatwright, J., and M. Cocco, Frictional constraints on crustal faulting, *J. Geophys. Res.*, *101*, 13,895-13,910, 1996.

Brace, W. F., and J. D. Byerlee, Stick-slip as a mechanism for earthquakes, *Science, 153*, 990-992, 1966.

Brune, J. N., Tectonic stress and the spectra of seismic shear waves from earthquakes, *J. Geophys. Res., 75*, 4997-5009, 1970.

Byerlee, J. D., Friction of rocks, *Pure Appl. Geophys., 116*, 615-625, 1978.

Cao, T., and K. Aki, Effect of slip rate on stress drop, *Pure Appl. Geophys., 124*, 515-530, 1986.

Chester, F. M., J. P. Evans and R. L. Biegel, Internal structure and weakening mechanisms of the San Andreas fault, *J. Geophys. Res., 98*, 771-786, 1993.

Chester, F. M., A rheologic model for wet crust applied to strike-slip faults, *J. Geophys. Res., 100*, 13,033-13,044, 1995.

Dieterich, J. H., Time-dependent friction in rocks, *J. Geophys. Res., 77*, 3690-3697, 1972.

Dieterich, J. H., Time-dependent friction and the mechanics of stick-slip, *Pure Appl. Geophys., 116*, 790-806, 1978.

Dieterich, J. H., Modeling of rock friction, 1, Experimental results and constitutive equations, *J. Geophys. Res., 84*, 2161-2168, 1979.

Dieterich, J. H., A model for the nucleation of earthquake slip, in *Earthquake Source Mechanics, Geophys. Monogr. Ser.*, Vol. 37, edited by S. Das et al., pp. 37-49, AGU, Washington, D.C., 1986.

Dieterich, J. H., and B. D. Kilgore, Direct observation of frictional contacts: New insights for state-dependent properties, *Pure Appl. Geophys., 143*, 283-302, 1994.

Ellsworth, W. L., Characteristic earthquakes and long-term earthquake forecasts: Implications of central California seismicity, in *Urban Disaster Mitigation: the Role of Science and Technology*, edited by F. Y. Cheng and M. S. Sheu, pp. 1-14, Elsevier Sci., New York, 1995.

Eshelby, J. D., The determination of the elastic field of an ellipsoidal inclusion, and related problems, *Proc. R. Soc. London, Ser. A., 241*, 376-396, 1957.

Fredrich, J. and B. Evans, Strength recovery along simulated faults by solution transfer processes, in Rock Mechanics, Proceedings of the 33rd U.S. Symposium, pp. 121-130, A. A. Balkema, Brookfield, VT., 1992.

Gomberg, J., N. Beeler, and M. Blanpied, On rate-state and Coulomb failure models, *J. Geophys. Res., 105*, 7857-7871, 2000.

Gu, Y., and T.-f. Wong, Effects of loading velocity, stiffness and inertia on the dynamics of a single degree of freedom spring-slider system, *J. Geophys. Res., 96*, 21,677-21,691, 1991.

Hanks, T. C., and H. Kanamori, A moment magnitude scale, *J. Geophys. Res., 84*, 2348-2350, 1979.

Heaton, T. H., Evidence for and implication of self-healing pulses of slip in earthquake rupture, *Phys. Earth Planet. Inter., 64*, 1-20, 1990.

Hickman, S. H., and B. Evans, Growth of grain contacts in halite by solution transfer; Implications for diagenesis, lithification, and strength recovery, In *Fault Mechanics and Transport Properties of Rocks*, ed. B. Evans and T.-f. Wong, pp. 253-280, Academic, San Diego, CA, 1992.

Hickman, S. H., and B. Evans, Kinetics of pressure solution at halite-silica interfaces and intergranular clay films, *J. Geophys. Res., 100*, 13,113-13,132,1995

Kanamori, H., and C. R. Allen, Earthquake repeat time and average stress drop, in *Earthquake Source Mechanics, Geophys. Monogr. Ser.*, vol. 37, edited by S. Das et al., pp. 227-236, AGU, Washington, D.C., 1986.

Karner, S.L., C. Marone, and B. Evans, Laboratory study of fault healing and lithification in simulated fault gouge under hydrothermal conditions, *Tectonophys., 277*, 41-55, 1997.

Karner, S. L. and C. Marone, Effects of loading rate and normal stress on stress drop and stick-slip recurrence interval, in *Geocomplexity and the Physics of Earthquakes, Geophys. Monogr. Ser.*, vol. 120, edited by J. B. Rundle et al., pp. 187-198, AGU, Washington, D.C., 2000.

Kato, N., K. Yamamoto, H. Yamamoto, and T. Hirasawa, Strain-rate effect on frictional strength and the slip nucleation process, *Tectonophysics, 211*, 269-282, 1992.

Keilis-Borok, V. I., On estimation of the displacement in an earthquake source and of source dimension, *Ann. Geofis., 12*, 205-214, 1959.

Lachenbruch, A. F., Frictional heating, fluid pressure and the resistance to fault motion, *J. Geophys. Res., 85*, 6097-6112, 1980.

Linker, M. F., and J. H. Dieterich, Effects of variable normal stress on rock friction: observations and constitutive equations, *J. Geophys. Res., 97*, 4923-4940, 1992.

Lockner, D. A., A generalized law for brittle deformation of Westerly granite, *J. Geophys. Res., 103*, 5107-5123, 1998.

Lockner, D. A., and P. G. Okubo, Measurements of frictional heating in granite, *J. Geophys. Res., 88*, 4313-4320, 1983.

Lockner, D. A., and N. M. Beeler, Premonitory slip and tidal triggering of earthquakes, *J. Geophys. Res.,104*, 20133-20151, 1999.

Marone, C. J., Scaling of static friction and the rate of fault healing with loading rate during the earthquake cycle, *Nature, 391*, 69-72, 1998a.

Marone, C. J., Laboratory-derived friction laws and their application to seismic faulting, *Annu. Rev. Earth Planet. Sci., 26*, 643-696, 1998b.

Marone, C., J. E. Vidale, and W. L. Ellsworth, Fault healing inferred from time dependent variations in source properties of repeating earthquakes, *Geophys. Res. Lett., 22*, 3095-3098, 1995.

McGarr, A., Some comparisons between mining-induced and laboratory earthquakes, *Pure Appl. Geophys., 142*, 467-489, 1994.

McGarr, A., On relating apparent stress to the stress causing earthquake fault slip, *J. Geophys. Res., 104*, 3003-3011, 1999.

McGarr, A., and J.B. Fletcher, Mapping apparent stress and energy radiation over fault zones of major earthquakes, *J. Geophys. Res.*, in press, 2001.

Nakatani, M., and H. Mochizuki, Effects of shear stress applied to surfaces in stationary contact, *Geophys. Res. Lett., 23*, 869-872, 1996.

Nadeau, R. M., and L. R. Johnson, Seismological studies at Parkfield VI: Moment release rates and estimates of source parameters for small repeating earthquakes, *Bull. Seismo. Soc. Am., 88*, 790-814, 1998.

Nadeau, R. M. and T. V. McEvilly, Fault slip rates at depth from recurrence intervals of repeating microearthquakes, *Science, 285*, 718-721, 1999.

Okubo, P. G., and J. H. Dieterich, Effects of physical fault properties on frictional instabilites produced on simulated faults, *J.Geophys. Res., 88*, 887-890, 1984.

Olsen, M. P., C. H. Scholz and A. Leger, Healing and sealing of a simulated fault gouge under hydrothermal conditions: Implications for fault healing, *J.Geophys. Res., 103*, 7421-7430, 1998.

Power, W. L., and T. E. Tullis, The relationship between slickenside surfaces in fine-grained quartz and the seismic cycle, *J. Struct. Geol., 11*, 879-893, 1989.

Press, W. H., B. P. Flannery, S. A. Teukolsky, and W. T. Vetterling, *Numerical Recipes: The Art of Scientific Computing*, Cambridge Uni. Press, New York, 1986.

Prescott, W. H., N. E. King, and G Guohua, Preseismic, coseismic and postseismic deformation associated with the 1984 Morgan Hill, California, earthquake, in *The 1984 Morgan Hill California Earthquake*, J. H. Bennett and R. W. Sherburne eds., 137-148, California Division of Mines and Geology Special Publication 68, 1986.

Rice, J. R., and Y. Ben-Zion, Slip complexity in earthquake fault models, *Proc. Natl. Acad. Sci. U.S.A., 93*, 3811-3818, 1996.

Rice, J. R., and A. L. Ruina, Stability of steady frictional slipping, *J. Appl. Mech., 50*, 343-349, 1983.

Rice J. R., and S. T. Tse, Dynamic motion of a single degree of freedom system following a rate and state dependent friction law, *J. Geophys. Res., 91*, 521-530, 1986.

Roy, M., and C. Marone, Earthquake nucleation on model faults with rate- and state-dependent friction: Effects of inertia, *J. Geophys. Res., 101*, 13,919-13,932, 1996.

Ruina, A. L., Slip instability and state variable friction laws, *J. Geophys. Res., 88*, 10,359-10,370, 1983.

Sammis C. G., and J. R. Rice, Repeating earthquakes as low-stress drop events at a border between locked and creeping fault patches, in press *Bull. Seismol. Soc. Am.*, 2001.

Savage J. C., and M. D. Wood, the relation between apparent stress and stress drop, *Bull. Seismol. Soc. Am., 61*, 1381-1388, 1971.

Schaff, D. P, G. C. Beroza, and B. E. Shaw, Postseismic response of repeating aftershocks, *Geophys Res. Lett., 25*, 4559- 4552, 1999.

Scholz, C. H., Microfracturing and the inelastic deformation of rock in compression, *J. Geophys. Res, 73*, 1417-1432, 1968a.

Scholz, C. H., Experimental study of the fracturing process in brittle rock, *J. Geophys., Res*, *73*, 1447-1454, 1968b.

Scholz, C. H., *The Mechanics of Earthquakes and Faulting*, Cambridge Uni. Press, New York, 1990.

Scholz, C. H., P. Molnar, and T. Johnson, Detailed studies of frictional sliding of granite and implications for the earthquake mechanism, *J. Geophys. Res.*, *77*, 6392-6406, 1972.

Scholz C. H., C. A. Aviles, and S. G. Wesnousky, Scaling differences between large interplate and intraplate earthquakes, *Bull. Seismol. Soc. Am.*, *76*, 65-70, 1986.

Sibson, R. H., Interactions between temperature and pore-fluid pressure during earthquake faulting and a mechanism for partial or total stress relief, *Nature*, *243*, 66-68, 1983.

Vidale, J. E., W. L. Ellsworth, A. Cole and C. Marone, Rupture variation with recurrence interval in 18 cycles of a small earthquake, *Nature*, *368*, 624-626, 1994.

Wong, T.-f., On the normal stress dependence of the shear fracture energy, in *Earthquake Source Mechanics, Geophys. Monogr. Ser.*, Vol. 37, edited by S. Das et al., pp. 1-11, AGU, Washington, D.C., 1986.

N. M. Beeler and S. H. Hickman, MS 977, U.S. Geological Survey, 345 Middlefield Road, Menlo Park, CA 94025. (nbeeler@usgs.gov)

T.-f. Wong, Department of Geosciences, State University of New York, Stony Brook, NY, 11794-2100.

(Received January 13, 2000; revised May 24, 2000;
accepted June 28, 2000.)